Title
A model-based approach for rainfall rate retrieval over the sea surface through rain radar

Authors
Capolino, F
Facheris, L
Giuli, D
et al.

Publication Date
1997-12-01

DOI
10.1117/12.298175

A model-based approach for rainfall rate retrieval over the sea surface through rain radar

F. Capolino[a], L. Facheris[b], D. Giuli[b], F. Sottili[c]

[a]Dipartimento di Ingegneria Elettronica, Università di Siena - Italy
[b]Dipartimento di Ingegneria Elettronica, Università di Firenze - Italy
[c]Magnetek S.p.A. - Terranuova Bracciolini (Arezzo) - Italy

ABSTRACT

Vertical rainfall profile retrieval based on reflectivity data collected by spaceborne rain radars can be improved through the techniques that exploit an estimation of the sea surface Normalised Radar Cross Section (NRCS) as an additional information. However, errors that can currently be made in predicting the sea surface NRCS may significantly affect their performance. Therefore, in this paper we first address the problem to evaluate the NCRS of the sea surface perturbed by rain, when observed at nadir. For this purpose, the dominant effect of ring waves generated by rainfall is considered. The joint effect of wind is also considered. The proposed model is based on the Full Wave Model (FWM) theory. Some comparisons are made with an alternative, less flexible model based on the Integral Equation Model (IEM) theory, and partial comparisons are also made with experimental data, which authorize to consider the proposed model well grounded and exploitable for application. Then, we show that the model can be usefully exploited to improve rainfall rate vertical profile retrieval over the sea surface, in the case of nadir looking, single frequency radars.

Keywords: Spaceborne rain radar, nadir observations, sea surface, electromagnetic models, Normalized Radar Cross Section, rainfall profiles.

1. INTRODUCTION

Spaceborne radars and suitable data processing techniques to provide rainfall rate estimates over the sea/ocean surface on a regular basis, as can be made available by a satellite platform, are gaining increasing interest. Algorithms that have been proposed in the literature for retrieval of the rainfall rate vertical profile exploit backscatter or attenuation estimates derived from radar measurements[1]. Several important sources of error can impair the vertical rainfall profile thus reconstructed. The main drawback of attenuation-based techniques is the heavy (and mostly unpredictable) additional attenuation due to the occurrence of the melting layer of precipitation. On the other hand, surface-referenced techniques perform better when they can exploit a reliable estimate of the power backscattered by the sea surface, but actually only a very rough estimate of it is often available. Furthermore, both kinds of techniques need to make use of relationships between specific attenuation and reflectivity (the so called k-Z relationships), that most times are not fully representative of the real connection between the physical parameters involved.

In this framework, it is reasonably expected that a well-grounded prediction of the backscattering behaviour of the sea surface, accounting for the joint perturbations due to wind and rainfall, can be usefully exploited to improve performance of existing techniques for estimating rainfall intensity over the sea surface by means of a spaceborne rain radar. Fur such a prediction, electromagnetic (e.m.) models are needed that can suitably represent also effects of rainfall on the Normalized Radar Cross Section (NRCS) of the sea/ocean surface. Signals backscattered from the sea are random processes depending on several physical phenomena, but mainly on wind- and rainfall-induced corrugation: it is worth mentioning that while the influence of wind on sea NRCS has been investigated in depth, the effects on it of rainfall are not yet well known. However, it has been assessed that the influence of rainfall on the sea NRCS is not negligible[2,3].

Attenuation based rainfall rate retrieval algorithms cope with at least four different basic errors: the radar calibration errors, the errors related to the uncertainty in the standard reflectivity-attenuation and reflectivity-rainfall rate relationships,

[1] For further author information -
F.C. email: capolino@alpha1.ing.unisi.it; Telephone: +39 0577 263619
L.F. email: facheris@ingfi1.ing.unifi.it; WWW: http://telemat.die.unifi.it/Labradar; Telephone: +39 55 4796274; Fax: +39 55 494569
D.G. email: giuli@ingfi1.ing.unifi.it; WWW: http://telemat.die.unifi.it/Labradar; Telephone: +39 55 4796370; Fax: +39 55 494569
F.S.: email: sdaniele@val.it; Telephone: +39 55 860223

the errors in the measurements of the total PIA (Path-Integrated Attenuation) related to the attenuation at the current range cell, and finally the error in the estimation of the surface reflectivity (when exploited). A number of single frequency algorithms have been proposed in the literature[4], aiming at minimizing the effects of some of the aforementioned errors. In this paper we refer to the kZS algorithm[5], which is to be considered as one of the most effective. This algorithm is practically insensitive to radar calibration errors and to errors related to PIA above the rainfall top; anyway, when PIA is high, the influence of such errors decreases. On the other hand, when PIA takes low values, the kZS algorithm becomes more sensitive to the accuracy of the surface reflectivity estimate.

In order to point out the influence of rain on the sea surface NRCS, in Section 2 we first outline a method recently devised to predict such NRCS when the surface is corrugated by the joint action of wind and rainfall[6]. Such prediction is based on the Full Wave Model (FWM)[7-11]. Through the FWM results, the relevance of rainfall induced corrugation in Ku band (the most commonly utilized by spaceborne rain radars) is highlighted. In Section 3 we briefly recall the principle of the kZS algorithm; referring to the same numerical simulation setup and comparison method developed by Marzoug and Amayenc5. Then we show that expected variations of NRCS, that the aforementioned e.m. model ascribes to rainfall, may cause significant errors in rainfall profile retrieval. In Section 4 we introduce a possible upgrade of the kZS algorithm - that is the "two cells" method - that exploits the prediction provided by the e.m. model to improve performance of the rainfall profile retrieval. Results of numerical simulations are finally presented in Section 5.

2. PHYSICAL CHARACTERIZATION OF THE SEA SURFACE CORRUGATED BY WIND AND RAINFALL

Let us consider a sea surface corrugated by wind and by the effects of raindrop splashes. Bliven et al. have shown that the crown and stalks phases, following raindrop splashes, are important features to be considered for analysing backscattering near grazing incidence angle, while ring waves are important for backscattering at incidence angles near nadir[3]. Here we consider only ring waves, and model them as a random process with characteristics similar to those of waves generated by wind.

2.1 Surface roughness induced by rain

The roughness of the water surface is modelled through a Gaussian height distribution, with variance $h_R^2(rms)$. Suppose then that a fraction of the kinetic energy of the falling drops is transferred to the water surface to generate ringwaves. An approximate relationship between the variance $h_R^2(rms)$ and the rainfall rate, can thus be obtained referring to experimental results carried out with artificial rain reported by Bliven et al.[3] In that experiment, a fixed raindrops size (2.8 mm diameter) was used with drops falling from 1 meter above the water surface, thus hitting the water surface with a lower velocity then the terminal velocity of real rain. Trying to extrapolate in some manner such results to the real case of raindrops falling with their true terminal velocity, we assumed that the kinetic energy of rainfall and the mean square height of the surface are linearly related, independently of the type of rainfall. In order to obtain a relationship between the rms height of the water surface and rainfall intensity accounting for terminal velocity of raindrops, we considered two models of Drop Size Distribution (DSD):

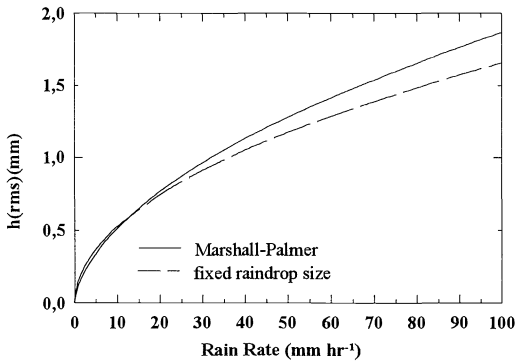

Fig. 1

a) a Dirac delta-shaped DSD centred on a fixed diameter of 2.1mm, which is close to the average real DSD maximum[3]
b) a Marshall-Palmer DSD.

It is reasonably believed that the simplifying assumption holds for 'normal' rainfall rates (R<100 mm/h): Fig. 1 reports the rms height $h(rms)$ versus rainfall rate obtained according to the aforementioned hypotheses. Notice that both DSDs considered lead to quite similar results, and that the rainfall intensity-rms height relationship obtained as above is not very sensitive to the adopted DSD model.

In order to provide a complete characterization of the water surface, intrinsically able to relate surface physical parameters to the NRCS, we adopted the ring wave frequency spectrum reported by Bliven et al.[12], converting it to the ring wave wavenumber spectrum - more suitable for e.m. models.

2.2 Surface roughness induced by wind

The contribution of blowing wind to total roughness is modelled as a zero mean Gaussian height distribution process. Two different wavenumber spectra were then considered: an approximated Pierson-Moscowitz spectrum as reported by Brown[13] and those reported in the more recent paper by Apel[14]. The distribution of the local surface slope has also been assumed as zero mean Gaussian, with variance calculated as in the papers by Bahar[9] and Bahar and Kubik[10], integrating the wavenumber spectrum.

2.3 E.m. modelling and validation of results

The model by Bahar[9] was utilized to obtain an accurate and complete polarimetric description of the sea surface echo power, under the influence of two statistically independent phenomena (wind and rainfall). The basic assumption is that total roughness is the superposition of two statistically independent random processes induced by rainfall and wind: spatially, the former is a large scale process, while the latter is a small scale process. In fact, the height standard deviation $h_{R(rms)}$ for the small scale process is of the order of a few millimetres, and its correlation length of the order of a few centimetres. Based on the values of wind roughness reported by Bahar[9] and Apel[14], it is easily verified that the average radius of curvature of the rain roughness is much larger than that of the wind roughness. If L_R and L_W are the correlation lengths of the roughness due to rain and to the wind, respectively, we have $L_W >> L_R$. Under these hypotheses, the small scale process 'rides' the large scale process.

As shown by Bahar and Kubik[10], when the mean slope is low, height distribution and slope distribution can be considered independent, which leads to a simplified formula for the NRCS. This is then calculated by means of a statistical average over the slopes and over the heights. The total NRCS σ is then written as[15]:

$$\sigma^{pq} = \int_{\bar{n}} A(\bar{n}^f, \bar{n}^i, n) Q(\bar{n}^f, \bar{n}^i, n) p(\bar{n}) d\bar{n} \tag{1}$$

with

$$Q(\bar{n}^f, \bar{n}^i, \bar{n}) = \left|\chi^R(\bar{v}\cdot\bar{n})\right|^2 Q_W(\bar{n}^f, \bar{n}^i) + (\bar{n}\cdot\bar{a}_y) Q_R(\bar{n}^f, \bar{n}^i, \bar{n}) \tag{2}$$

where we adopted the same definitions and symbols by Bahar[9]: in particular, *pq* represents the arbitrary polarization of incident and radiated waves (H,V) and the symbols. The term $A^{pq}(\bar{n}^f, \bar{n}^i, \bar{n})$ includes the Fresnel reflection coefficients, while $\left|\chi^R(\bar{v}\cdot\bar{n})\right|$ and $Q_{W,R}$ account for the statistics of the phase of the e.m. wave determined by the height distribution of the rough surface induced by wind and rain corrugations, respectively: for their expressions, the reader is referred to the work by Bahar[9]. The integration with respect to $\bar{n}$ means that the result is averaged along the slopes of the large scale surface due to the wind ($\bar{n}$ is the local normal to the large scale surface, and $p(\bar{n})$ is the Gaussian pdf of slopes). Notice that $Q_R(\bar{n}^f, \bar{n}^i, \bar{n})$ is weighted by the slope of the large scale surface while Q_W is not since, as mentioned above, it is assumed that the small scale corrugation rides the large scale corrugation. This corresponds to computing the ring waves contribution as a statistical average over the slopes of the wind roughened surface. Shadowing effects were not considered, since they are not relevant for observation angles close to nadir.

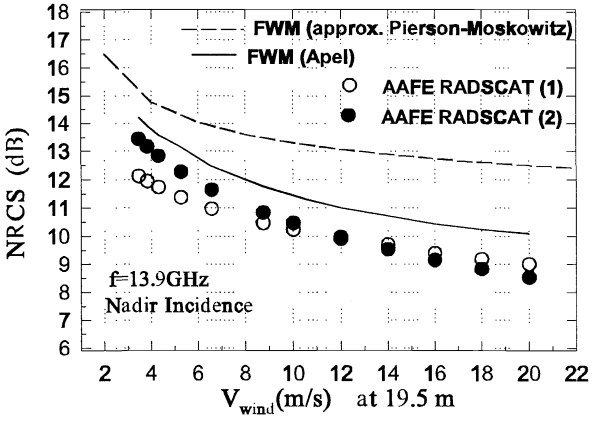

Fig. 2

In order to verify in first place the applicability of the FWM to the case of interest and, secondarily, the validity of the physical characterization of the sea surface, we compared the NRCS obtained by the FWM with that obtained by the Integral Equation Model (IEM)[16] in the case of corrugation induced by rainfall only, and with experimental results in the case of corrugation induced by wind only.

In the first case, considering only ring waves, we found that the sea surface NRCS predicted by FWM is in a very good agreement with that predicted by IEM for several rms heights $h_{R(rms)}$ and incidence angles considered[6]. In the second case

(wind corrugation only) we compared the predicted NRCS with the experimental results by Schroeder et al.[17] obtained at 13.9 GHz . In Fig. 2 we compare such experimental data, taken from the regression line reported by Schroeder et al.[17], together with the curves (relative to nadir incidence) for two wavenumber spectra considered, namely the approximated Pierson-Moskowitz and the Apel spectra. The measurements have been carried out in two distinct experiments.

As expected, the Apel spectrum fits better the actual NRCS behaviour. Notice that the calculated NRCS is slightly higher than the measured one. Also Schroeder et al.[17] noticed this effect by comparing their measurements with the SASS I model, and couldn't explain it. However, this difference is of the order of the uncertainity of the measurements, and could also be imputed to the Apel spectrum. The approximated Pierson-Moskowitz spectrum is not so accurate for nadir incidence; though, we found that its prediction off from nadir is in rather good agreement with the experimental results[6].

The results we report, accounting for both wind and rainfall corrugation, refer to 13.75 GHz operating frequency and to 4.3 m/s wind speed (as in Bahar and Fitzwater[7]). The surface corrugation contributed by rainfall is expressed in terms of standard deviation $h_R(rms)$, since this is related to rainfall rate through the approximated law of Fig. 1. Nevertheless, an accurate description of such relationship is not available in the literature: for this reason, we have simply chosen h_R as the parameter describing sea roughness and rainfall intensity; one can obtain the NRCS as a function of h_R using Eqs. (1) and (2). In Fig. 3, the VV NRCS response is plotted versus the incidence angle in the absence of rainfall, and in the case that additional perturbation due to rainfall is present, for different values of the surface roughness. When increasing rainfall intensity (i.e. increasing $h_R(rms)$), a decrease of the NRCS is correspondingly obtained for incidence angles close to nadir; this phenomenon can be observed for all incidence angles ranging from 0° to 10°. On the other hand, at incidence angles ranging from around 10° to 35° an opposite behaviour is evident, i.e. for increasing intensity a corresponding increase of the sea surface NRCS shows up, as also observed in the laboratory experiment by Bliven et al.[3]. At this frequency, NRCS is rather sensitive to rainfall intensity.

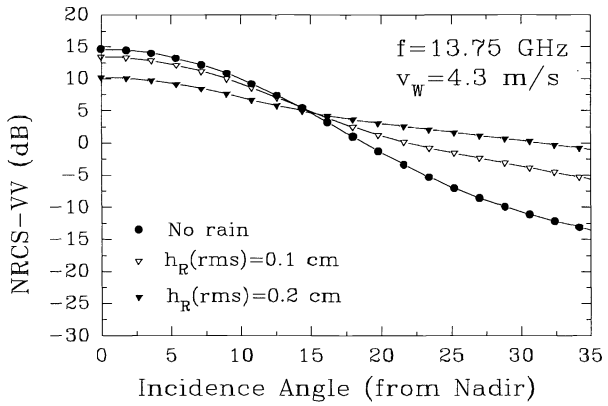

Fig. 3

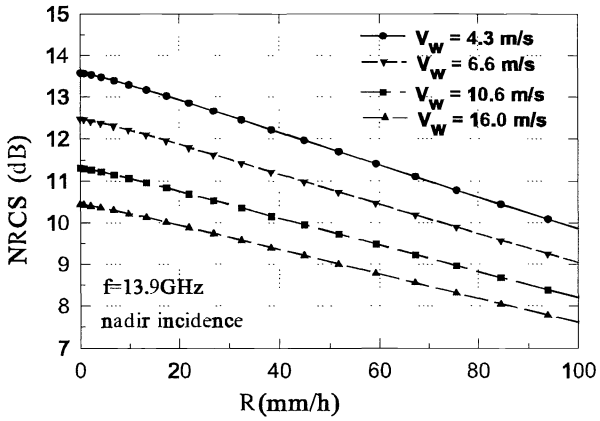

Fig. 4

In Fig. 4 we report the sea surface NRCS versus rainfall rate R for some wind speeds and nadir incidence obtained using the more accurate Apel spectrum. Notice that the variations ascribable to rainfall rate are of the same order of magnitude as those due to wind speed: this justifies the inclusion of rainfall induced corrugation in the e.m. model.

As a last remark concerning model adequacy, we must point out that heavy rainfall may have the effect of damping sea waves, causing an increase of the NRCS at nadir incidence[18], which is not accounted for by the adopted e.m. model. Indeed, the combined effects of damping and of impact-induced corrugation due to rainfall deserve further investigations, although sensitivity of the kZS algorithm to sea NRCS errors decreases with increasing rainfall rate. We notice also that, in the presence of damping effects, ring waves as accounted for by the adopted e.m. model, should probably play a dominant role at Ku band, being their size comparable with the e.m. wavelength.

3. PRINCIPLE OF THE KZS ALGORITHM

We recall here for convenience the basic principle of the kZS algorithm, proposed by Marzoug and Amayenc to estimate rainfall rate vertical profiles with a nadir-looking radar[5]. The algorithm exploits the ratio between the power backscattered from a generic resolution cell ranging r from a nadir looking spaceborne radar that operates at attenuating frequency, and the power backscattered by the resolution cell that includes the sea surface. The limiting assumption of the nadir incidence

angle is needed to ensure that the sea surface radar return is dominant in the total return of the latter volumetric radar resolution cell only, thus avoiding that surface return contaminates significantly the former cell, even through antenna sidelobes.

The algorithm exploits power estimates and standard reflectivity-attenuation relationships to provide the vertical profile of specific attenuation, through which the rainfall rate profile is in turn estimated. As shown below, the power ratio instead of the absolute power is exploited, utilizing the sea surface as the starting point in the integration of radar measurements, leading to the vertical attenuation profile estimate. This approach avoids bias errors such as those made by integrating power estimates from the melting layer, or absolute system calibration errors.

Analytically, the ratio is made between the mean power, $\overline{P(r)}$, of the rain echo from the volume centred at range r (in km) from the radar, proportional to the rain reflectivity factor $Z(r)$ and to the attenuation factor along the path:

$$\overline{P(r)} = \frac{C}{r^2} Z(r) \exp\left[-0.46 \int_0^r k(s) ds \right] \tag{3}$$

and the mean power, $\overline{P_s(r_s)}$, backscattered by the sea surface located at distance r_S from radar, which is proportional to the sea surface NRCS (referred to as σ_s):

$$\overline{P_s(r_s)} = \frac{C_s}{r_s^2} \sigma_s \exp\left[-0.46 \int_0^{r_s} k(s) ds \right] \tag{4}$$

The overbar indicates mean value, $k(s)$ is the specific attenuation coefficient (dB/km) at range s, for e.m. propagation through rainfall, while C and C_S are the radar constants accounting for system parameters in the volume and surface backscatter cases, respectively. Assuming that attenuation is due exclusively to rainfall, Z and k are tied by a standard empirical relationship of the kind:

$$Z(r) = \alpha(r) \cdot k^{\beta}(r) \tag{5}$$

where α and β depend on frequency and Drop Size Distribution (DSD). β is supposed to be constant and known along the path, while α is considered as varying with range. Introducing this relationship in Eq. (3), the ratio $\overline{P(r)} / \overline{P_s(r_s)}$ gives, after simple manipulations:

$$k(r) \exp\left(\frac{0.46}{\beta} \int_r^{r_s} k(s) ds \right) = w_0(r) \tag{6}$$

where

$$w_0(r) \stackrel{\Delta}{=} \left[\frac{\overline{P(r)} \cdot r^2 \sigma_s C_s}{\overline{P_s(r_s)} \cdot r_s^2 \alpha(r) \cdot C} \right]^{1/\beta} \tag{7}$$

With respect to $g(r) \stackrel{\Delta}{=} \exp\left(\frac{0.46}{\beta} \int_r^{r_s} k(s) ds \right)$, Eq. (6) is a first order differential equation whose solution implicitly gives $k(r)$:

$$k(r) = w_0(r) \Big/ \left[1 + \frac{0.46}{\beta} \int_r^{r_s} w_0(s) ds \right] \tag{8}$$

The rainfall rate profile $R(r)$ can then be obtained from $k(r)$ by means of a frequency-dependent relationship of the kind $R(r) = Ak(r)^B$. Eq. (8) shows that the estimate of $k(r)$ provided by the kZS is not sensitive to the characteristics of precipitation at ranges less than r. In particular, if r refers to a radar cell below the melting layer, no assumption about its structure is needed a priori when using the kZS algorithm.

The function $w_0(r)$ increases with increasing attenuation along the path between the surface and the range cell at distance r from the radar. This causes a lower sensitivity to σ_s. On the other hand, when attenuation is low, sensitivity to σ_s becomes relevant.

In this regard, an important problem comes along: the actual NRCS of the sea surface σ_s is a priori largely unknown, while it needs to be best approximated in the algorithm. To cope with this problem, an improved guess value of σ_s could be inferred, for instance, from measurements made over near regions where the sea surface is similarly perturbed by wind, and rainfall is absent, while local perturbation due to rainfall is accounted for by a sea surface model.

The guess value of σ_s, to be used in the kZS algorithm, will be hereafter referred to as σ_o. A systematic (mean) error σ_B (which may also take negative values) is introduced, depending on the way σ_o is determined:

$$\sigma_s = \sigma_o + \sigma_B \tag{9}$$

When σ_o does not account for changes of sea surface NRCS due to surface wind and to rainfall perturbations, remarkable values of σ_B can occur in actual cases, which directly affect the efficiency of the rainfall profile reconstruction.

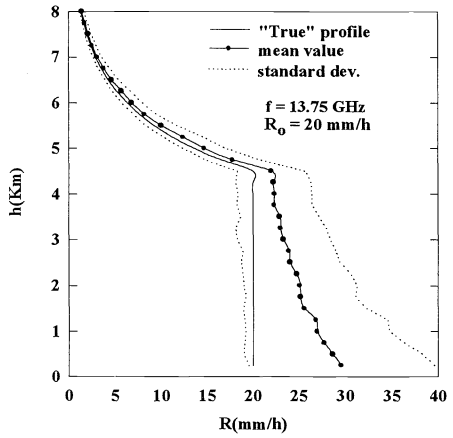

Fig. 5

With the purpose to demonstrate the effectiveness of the kZS algorithm, Marzoug and Amayenc simulated spaceborne radar measurements based on the acquisition of 60 independent echo samples[5]. Referring to a 'true' rainfall profile, 100 profiles were reconstructed by means of the kZS algorithm, accounting for all possible errors cited in Section 1, in order to evaluate their influence.

Resorting to a fixed mean value for the sea surface NRCS is indeed the only solution when no other data are available but rain radar measurements. In their simulations, Marzoug and Amayenc assumed a "climatological" guess value σ_o=12 dB at 13.75 GHz, which can be approximately considered the mean value of sea NRCS with respect to wind speed variations[19]. In this situation, as evidenced by Fig. 4, σ_B=3dB can reasonably be considered a potential (not maximum) value of the bias error, suitable to evaluate performance degradation of the kZS algorithm. In this regard, Fig. 5 shows the error made utilising the kZS algorithm as a function of altitude for σ_s=9 dB and σ_o=12 dB, and a rainfall rate of 20 mm/h at the sea surface level. Notice that the relative error (i.e. the ratio between the standard deviation and the mean value of the estimated rainfall rate at a given altitude) falls around 50% in the lower region. A still increased error is expected when NRCS variations due to rainfall are not accounted for by σ_o: according to Fig. 4, for a maximum expected R=100 mm/h, the maximum NRCS bias due to rainfall is about 3 dB, almost independently of wind speed.

4. ESTIMATING RAINFALL RATE AT SEA LEVEL: THE "TWO CELLS" METHOD

The simple method introduced in this Section predicts both sea NRCS and rainfall rate over the sea surface, by exploiting the proposed e.m. model. We will refer to it as the "two cells" method, since it accounts only for echoes from a couple of adjacent radar range cells, namely those closest to the sea surface. For simplicity, suppose that range sidelobes are sufficiently low, so that interference among contiguous range cells can be neglected.

Two basic assumptions are needed:

1) the contribution of the sea surface to the first cell return, at range r_s, is much more powerful than that due to rainfall;
2) rainfall rate is the same in the two adjacent range cells.

Under such hypotheses, if Δr is the range resolution, $\overline{P_s}$ and $\overline{P}$ the mean powers related to the first cell (including the sea surface) and the second cell (centered at range r), respectively, we get ($r/r_s \approx 1$):

$$\frac{\overline{P_s}}{\overline{P}} = \frac{C_s \cdot \sigma_s(R) \cdot e^{-0.46 \Delta r\, k(R)}}{C \cdot Z(R)} \tag{10}$$

where $\sigma_s(R)$ expresses the sea NRCS dependence on the rainfall rate R. Exploiting Eq. (5), we obtain:

$$\left(\frac{\alpha(r_s)\cdot\overline{P_s}\cdot C}{\overline{P}\cdot C_s}\right)^{1/\beta} = \frac{\sigma_s(R)^{1/\beta}\cdot e^{-0.46\frac{\Delta r}{\beta}k(R)}}{k(R)} = f(R)\,. \tag{11}$$

To estimate rainfall rate in the proximity of the sea surface, $f(R)$ in the previous equation can be inverted with respect to R ($f(R)$ is a monotonic decreasing function), once good estimates of $\overline{P_s}$, $\overline{P}$ and $a(r_s)$, as well as of the radar constants C and C_S are available. On the other hand, the actual relationship $\sigma_s(R)$ is unknown. The e.m. model can thus be exploited to provide the 'guess' law $\sigma_o(R)$ to be introduced in Eq. (11) in place of $\sigma_S(R)$..

While this method estimates rainfall rate based on two mean power estimates, the e.m. model predicts the NRCS as a function of wind speed and rainfall rate. Indeed, the estimate may suffer from the approximations introduced through the conditions 1) and 2) mentioned above. Interference problems between surface and volumetric echoes deriving from echo pulse spreading induced by beamwidth, rough surface and limited system bandwidth could be overcome by applying the "two cells" method to a couple of not adjacent range cells. Obviously, exploiting this flexibility of the method needs the stronger assumption of constant rainfall in a higher column over the sea surface. However, the alternative would be to tolerate a priori a residual NRCS bias in the standard kZS algorithm. Summarizing, the following steps should be followed for an accurate estimation of the rainfall profile in the framework described:

1) Utilize a measured, estimated or predicted value of wind velocity over the sea surface;
2) for that wind velocity, select the theoretical relationship between rainfall rate R and surface NRCS;
3) utilize the "two-cells" method to provide a rainfall rate estimate over the sea surface, jointly with the related NRCS estimate;
4) utilize the NRCS estimate in the kZS algorithm for rainfall profile retrieval.

5. ERROR PARAMETERS AND SIMULATION RESULTS

As a matter of fact, the *Z-k,* the *Z-R* and the $\sigma_s(R)$ relationships utilized are affected by several uncertainties. With the purpose to compare the results of the simulated reconstructions with some 'truth' reference, we regarded all the aforementioned relationships as deterministic references; in particular, we assumed the 'true' law $\sigma_s(R)$ to coincide with $\sigma_o(R)$ provided by the FWM. Then, the random error parameters described below were used to simulate uncertainties related to those relationships and to radar power estimates, and to write a modified version of Eq.(11). This was done by utilizing the error parameters utilized by Marzoug and Amayenc for the kZS algorithm[5]. They are briefly recalled below:

1) Referring to the basic Marshall Palmer DSD model $N(D)=N_o exp(-\Lambda D)$, the remarkable random variations that N_0 may undergo along the propagation path are accounted for by substituting N_0 with the following random variable N_{0m}:

$$N_{0m} = \nu N_0 \tag{12}$$

where ν is a unitary mean value random variable with Gamma pdf and 0.5 standard deviation.

2) The 'measured' powers P_m and P_{Sm} are related to the mean powers as follows:

$$P_m = \delta_r \overline{P} \qquad \text{and} \qquad P_{S\,m} = \delta_S \overline{P_S}\,. \tag{13}$$

where δ_r and δ_S are random variables accounting for the estimation errors related to cells where rainfall echo and surface echo is prevailing, respectively. If N_i independent samples are integrated, the pdf of both random variables is:

$$p(x) = N_i^{N_i} x^{N_i-1} exp(-N_i x)/(N_i-1)! \tag{14}$$

3) The variability of N_0 is considered as the only source of uncertainty in the following relationships between the the specific attenuation k, the rainfall rate R and the reflectivity Z:

$$Z = EN_0^{1-b}R^b \qquad k = FN_0^{1-d}R^d \qquad Z = EF^{-\beta}N_0^{1-\beta}k^\beta \tag{15}$$

where E, F, b, d depend on frequency and $\beta=b/d$. In the third of Eqs. (15), $EF^{1-b}N_o^{1-b}$ corresponds to a of Eq.(5). The uncertainty on α is accounted for by substituting it with the random variable α_m defined as follows:

$$\alpha_m = \alpha_1 \alpha \tag{16}$$

where α_1 is a random variable that, from Eqs. (5) and (15), can be expressed as $\alpha_1 = v^{1-\beta}$.

A discussion apart is opportune about uncertainties affecting the estimate of the sea NRCS. As done by Marzoug and Amayenc, these have been accounted for, by the random variable σ_m defined as follows:

$$\sigma_m = \sigma_1 \cdot \sigma_o \tag{17}$$

where σ_1 represents the uncertainty in the 'guess' value defined by Eq. (9), and is modeled through a Gamma pdf with unitary mean value and 0.5 standard deviation. Marzoug and Amayenc observed that they had neglected "possible systematic changes in σ_o due to the effects of raindrops impinging on the ocean surface or to the effects of surface winds"[5]. Consequently, the random variable σ_1 represented random fluctuations around the fixed value σ_o, and that was made to account mainly for NRCS variations from one profile to another. Since the guess law $\sigma_o(R)$ provided by the e.m. model discussed here does accounts for both the corrugations due to wind and rainfall, we assumed $\sigma_B=0$ in our simulations. With these premises, using for σ_1 the same relative standard deviation (50%) that they used, basically corresponds in this new context to assuming rough (and/or area-averaged) wind estimates. Secondarily, σ_1 may also account for a residual percentage of error related to the e.m. model approximations. Notice therefore that the simulations results turn out to be pessimistic in case reliable wind estimates are available, in particular when obtained with good spatial and temporal resolution.

Accounting for the error parameters and exploiting Eq. (6), the 'measured' function corresponding to $w_0(r)$ is:

$$w_{0m}(r) = \left(\frac{\delta_r(r) \cdot \overline{P(r)} \cdot r^2 \sigma_1 \sigma_0 C_s}{\delta_s \overline{P_s(r_s)} \cdot r_s^2 \alpha_1 \alpha \cdot C} \right)^{1/\beta} = w_0(r) \cdot T(r) \tag{18}$$

where $T(r)$ is a random process, function of r:

$$T(r) = \left(\frac{\sigma_0 \delta_r(r) \sigma_1}{\sigma_S \delta_s \alpha_1} \right)^{1/\beta} \tag{19}$$

and $\delta_r(r)$ accounts for variations along the propagation path of the mean power estimate errors. These errors are supposed independent from one range cell to the other. The 'estimated' attenuation factor $k_m(r)$ becomes therefore:

$$k_m(r) = k(r) \cdot T(r) \cdot exp\left(\frac{0.46}{\beta} \int_r^{r_s} k(s) ds \right) \Bigg/ 1 + \frac{0.46}{\beta} \int_r^{r_s} k(s) \cdot T(s) \cdot exp\left(\frac{0.46}{\beta} \int_s^{r_s} k(t) dt \right) ds \tag{20}$$

and the final expression relating the 'estimated' rainfall rate $R_m(r)$ to the 'true' rainfall reference $R(r)$ is:

$$R_m(r) = R(r) \left[\frac{v^{d-1} T(r) \cdot exp\left(\frac{0.46}{\beta} FN_0^{1-d} \int_r^{r_s} R(s)^d ds \right)}{1 + \frac{0.46}{\beta} FN_0^{1-d} \int_r^{r_s} R(s)^d T(s) exp\left(\frac{0.46}{\beta} FN_0^{1-d} \int_s^{r_s} R(t)^d dt \right) ds} \right]^{1/d} \tag{21}$$

Finally, exploiting Eqs. (5) and (15) to modify Eq. (11), and including in it all factors of uncertainty and errors considered, one gets the following expression, which implicitly defines the 'measured' rainfall rate R_m at the sea level:

$$\frac{\delta_s \cdot \overline{P_s} \cdot C}{\delta_r \cdot \overline{P} \cdot C_s} = \frac{\sigma_1 \sigma_0(R_m) \cdot e^{-0.46 \Delta r F N_{0m}^{1-d} R_m^d}}{E N_{0m}^{1-b} R_m^b} \tag{22}$$

Introducing the ratio $\overline{P_s} / \overline{P}$ as from Eq. (10), utilizing the 'guess' law $\sigma_o(R)$ and exploiting again Eqs.(15), one gets the expression that has been utilized in the simulations to provide R_m.:

$$\frac{\sigma_1 \sigma_0(R_m) \cdot e^{-0.46 \Delta r F N_0^{1-d} v^{1-d} R_m^d}}{v^{1-b} R_m^b} = \frac{\delta_s \sigma_0(R) \cdot e^{-0.46 \Delta r F N_0^{1-d} R^d}}{\delta_r R^b} \tag{23}$$

In the simulations, we assumed that 60 independent echo samples were integrated in correspondence of each range cell. A given vertical profile of rainfall rate was then assumed as the 'truth' reference. Referring to 13.75 GHz, we used Eqs. (15) as 'true' relationships with the values[4] E=0.66 10^6, b=1.5, F=0.309 and d=1.156.

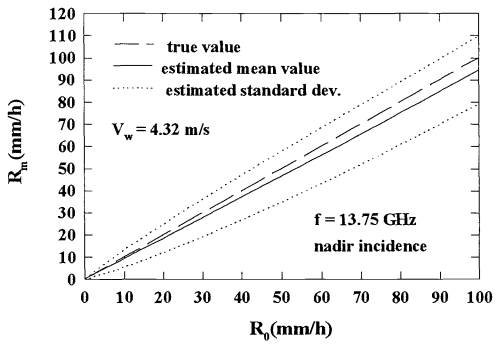

Fig. 6

A first kind of analysis of simulated data concerned the accuracy of R_m estimated through Eq. (22). 100 independent 'estimations' of R_m were performed, based on the same error statistics and on the same rainfall profile. Fig. 6 plots the 'true' rainfall rate (R) at the sea level versus the rainfall rate estimate (R_m) thus obtained. A wind velocity of 4.32 m/s at 19.5 metres of altitude is assumed. Two additional curves corresponding to the estimated standard deviation of R_m are also plotted, together with the curve reporting the exact profile (i.e. that would be reconstructed if random errors were absent). Notice that the absolute error increases with increasing rainfall rate, but the relative error is practically constant.

As far as rainfall profile retrieval is concerned, referring to analogous simulations[5] we first considered a rainfall profile with a constant rainfall rate up to an altitude of 4.5 km, then decreasing with a corresponding reflectivity decrease rate of 5 dB/km. A rainfall rate of 10 mm/h at the sea level was considered, assuming the aforementioned wind velocity. In Fig. 7 the reconstructed rainfall profile is shown. Mean value and standard deviation of 100 independent reconstructions are plotted for the 32 range cells (range resolution: 250 m) up to an altitude of 8 Km.

Fig. 8 shows the rainfall profile reconstructed assuming a rainfall rate at the sea level of 50 mm/hr. A good estimate is achieved also in this case at all altitudes. Notice also that in correspondence of higher rainfall rates estimate accuracy improves thanks to an increased attenuation. Fig. 9 shows similar results, corresponding to a wind velocity of 20 m/s and a rainfall rate at sea level of 10 mm/hr. Comparing such results with those of Fig. 7, the conclusion can be drawn that remarkable variations of wind velocity do not influence significantly the accuracy of profile retrieval (assuming the same accuracy for wind measurements). Reflectivity gradients that are generated immediately over the sea surface may affect the rainfall profile retrieval. Therefore, in other simulations we employed a different rainfall profile, with a gradient below 4.5 Km altitude corresponding to a reflectivity loss rate of 1 dBZ/Km, and a rainfall rate of 50 mm/hr at that altitude. The results, at 13.75 GHz and with a wind of 4.3 m/s, are shown in Figs. 10 and 11 for negative and positive reflectivity gradients, respectively. The reconstruction performance is extremely good in terms of mean values also in these cases of rainfall variable with height immediately above the sea surface; furthermore, notice that it is accompanied by an accuracy comparable with that of Fig. 9, which depends primarily on the top rainfall intensity of 50 mm/h.

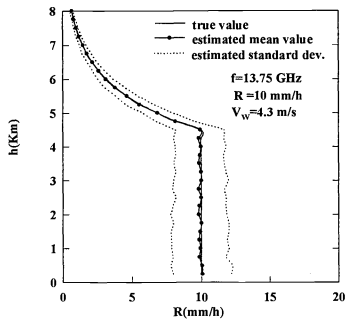

Fig. 7

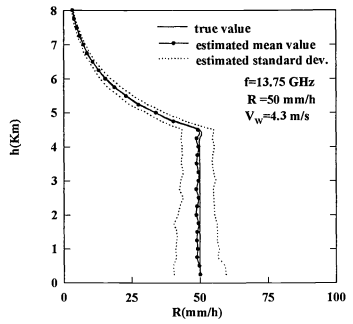

Fig. 8

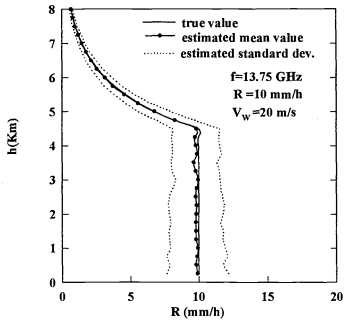

Fig. 9

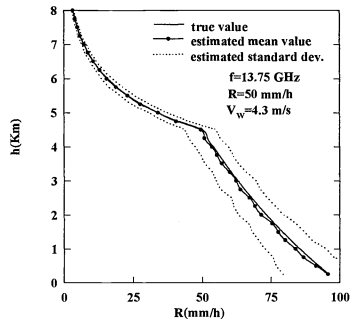

Fig. 10

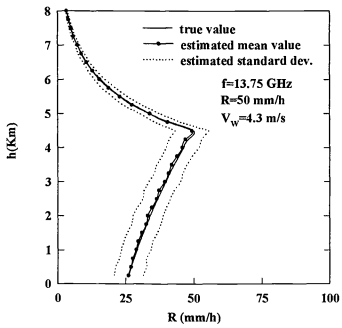

Fig. 11

6. CONCLUSIONS

We highlighted that a direct use of the kZS algorithm with an excessively approximated guess of the sea NRCS can cause relevant errors in the reconstructed rainfall profiles. A more accurate guess of such NRCS can be provided by an e.m. model such as the FWM, purposely adapted. In this framework, we also pointed out that sea surface roughness induced by rainfall cannot be neglected by a model-based predictor. In particular, through the aforementioned e.m. model it is possible to derive, in the general case of a sea surface corrugated by wind and rain, a relationship between surface NRCS and rainfall rate at nadir incidence, as a function of surface wind velocity. In spite of the intrinsic residual approximations of such a model, the derived relationship confirms that rainfall remarkably modifies the NRCS value that would be predicted accounting for wind only. We neglected the damping effects of sea waves, which may appear in the presence of quite heavy rainfall: this aspect obviously deserves further investigations for the refinement of the prediction model, but it requires basically a quite complex hydrological analysis of sea surface - raindrops interactions. Anyway, errors induced by the damping effects of sea waves due to rainfall should be attenuated by a reduced sensitivity of the kZS algorithm to the NRCS estimate errors in the case of heavy rainfall.

By means of the "two cells" method it is then possible to get directly estimates of rainfall rate and NRCS referred to the sea surface. While the latter estimate can then be utilized to improve performance of the kZS algorithm, the former estimate provides a direct estimate of the rainfall rate in proximity to the sea surface. Improved performance in rainfall rate profile retrieval has been demonstrated by means of numerical simulations, carried out at 13.75 GHz for different values of wind velocity, different rainfall rates over the sea surface and different rainfall profiles. All of them showed that the rainfall profile retrieval accuracy can greatly benefit from a more accurate prediction of NRCS. This requires that wind velocity over the area of interest is available, provided by either measurements or models, or joint exploitation of both of them. Additional measurements should refer to the same or a contiguous area, provided by an independent sensor, such as a scatterometer. In

summary, the proposed method could be profitably exploited in all those contexts where some additional information allows to overcome the bare hypothesis of a generic 'standard' average value of sea NRCS.

ACKNOWLEDGEMENTS

This work has been supported by the Italian Space Agency, with partial contribution of the Italian Ministry for University and Scientific Research. The authors would also like to thank Prof. P. Sobieski for useful discussions.

REFERENCES

1. Iguchi, T., R. Meneghini: "Intercomparison of Single-Frequency Methods for Retrieving a Vertical Rain Profile from Airborne or Spaceborne Radar Data", *Journ. of Atmosph. Oceanic Techn.* V.11, pp-1507-1516, 1994.
2. Moore, R.K., Y.S. YU, A.K. Fung, D. Kaneko, G.J. Dome, and R.E. Werp: "Preliminary study of rain effects on radar scattering from water surface", *IEEE Journ. Oceanic Eng.*, V.9, 364-382, 1979.
3. Bliven, L.F., H. Branger, P. W. Sobieski and J-P Giovanangeli, "An Analysis of Scatterometer Returns from a Water Surface Agitated by Artificial Rain: Evidence that Ring-Waves are the Main Feature", *Int. Journ. Remote Sensing.*, V.14, N.12, pp.2315-2329, 1993.
4. Marzoug, M., P. Amayenc: "A Class of Single- and Dual-Frequency Algorithms for Rain Rate Profiling from a Spaceborne Radar. Part I: Principle and Test from Numerical Simulations", *Journ. Atmos. Ocean. Remote Sensing.*, V.11, pp. 1480-1506, December 1994.
5. Marzoug, M., P. Amayenc: "Improved Range-Profiling Algorithm of Rainfall Rate from a Spaceborne Radar with Path-Integrated Attenuation Constraint", *IEEE Trans. Geoscience and Remote Sensing*, V.29, N.4, pp.584-592, July 1991.
6. Capolino, F., L. Facheris, D. Giuli, F. Sottili: "E.M. models for evaluating rain perturbation on the NRCS of the sea surface observed near nadir", *Submitted to IEE Proceedings Radar, Sonar and Navigation*
7. Bahar, E., M. A. Fitzwater: "Scattering Cross Section for Composite Rough Surfaces Using the Unified Full Wave Approach", *IEEE Trans. Antennas and Propag.*, V. AP-32, N. 7, 730-734, July 1984.
8. Bahar, E., M. A. Fitzwater: "Like- and cross- polarized scattering cross sections for random rough surfaces: theory and experiment", *J. Opt. Soc. Am.,* A-2, 2295-2303, 1985.
9. Bahar, E.: "Review of the Full Wave Solutions for Rough Surface Scattering and Depolarization: Comparisons with Geometric and Physical Optics, Perturbation, and Two-scale Hybrid Solution", *Journ. Geophysical Res.*, V. 92, N. C5, 5209-5224, May 1987.
10. Bahar, E. , R. D. Kubik: "Tilt Modulation of High Resolution Radar Backscatter Cross Sections: Unified Full Wave Approach", *IEEE Trans. on Geosci. Rem. Sens.*, V. 31, N. 6, 1229-1242, Nov. 1993.
11. Bahar, E., and Y. Zhang: "A New Unified Full Wave Approach to Evaluate the Scatter Cross Section of Composite Random Surfaces", *IEEE Trans. on Geoscience and Remote Sensing*, V.34, 973-980, July 1996.
12. Bliven, L.F., P. W. Sobieski, T. Elfouhaily: "Ring Wave Frequency Spectra: Measurements and Model", *Proc. IGARSS'95*, Florence, July 1995, pp.830.
13. Brown G S, "Backscattering from a Gaussian distributed perfectly conducting rough surface", *IEEE Trans. Antennas and Propag.*, 26, N.3, pp.472-482, 1978.
14. Apel, J. R.: "An improved model of the ocean surface wave vector spectrum and its effects on radar backscattering", *Journ. of Geophys. Research,* V. 99 N. C8, pp 16,269-16,291, August 1994.
15. Capolino, F., L. Facheris, D. Giuli., F.Sottili: "Estimating RCS of the Sea Surface Perturbed by Rain for Rainfall Rate Retrieval", *Proc. IGARSS'96*, Lincoln, Nebraska, May 1996, pp. 13-15.
16. Fung A K, Li Z, Chen K S, "Backscattering from a randomly rough dielettric surface", *IEEE Trans. Geoscience and Remote Sens.*, 30, pp.356-369, 1992.
17. Schroeder L C, Schaffner P R, Mitchell J L, Jones W L, "AAFE RADSCAT 13.9-GHz Measurements and Analysis: Wind-Speed Signature of the Ocean", *IEEE Journ. Ocean. Eng.*, 10, N.4, pp.346-357, 1985.
18. Durden S L., Haddad Z S, Im E, Kitiyakara A, Li F K, Tanner A B and Wilson W J, "Measurement of rainfall path attenuation near nadir: A comparison of radar and radiometer methods at 13.8 GHz", *Radio Science*, 30, N. 4, pp. 943-947, 1995.
19. Manabe, T. and T. Ihara: "A Feasibility Study of Rain Radar for the Tropical Rainfall Measurement Mission. Part. 5: Effects of Surface Clutter on Rain Measurements from Satellite", J. Commun. Res. Lab., V.35, N.145, 163-182, 1988.